Detrimental Effects of Dust Deposition in Pores of an Open Volumetric Air Receiver

Gurveer Singh[1] and Laltu Chandra[1#]

[1]Indian Institute of Technology Jodhpur, Jodhpur (India)

[#] corresponding author: chandra@iitj.ac.in

Abstract

Recently the novel concept of solar convective furnace based on open volumetric air receiver is proposed and evaluated for metals processing. The use of open volumetric air receiver is motivated by the need of hot air at about 750 K. It is well-accepted that the dust deposition will be a major challenge for implementation of open volumetric air receiver in the arid deserts, worldwide. In this paper, some of its detrimental consequences pertaining to flow instability and absorber temperature are presented. A pressure-drop correlation for straight pore based absorber is developed for analyzing the flow instability. A two-dimensional validated approach is adopted for analyzing the receiver overheating as a result of dust deposition forming a so-called insulation-type layer on the inner surface of absorber pore. The findings show stable flow regime with a uniform thickness of the deposited dust layer (100 µm & 200 µm) on the inner surface of a pore. The thickness of dust layer is more detrimental in view of substantial rise of absorber temperature and thus, the sustainability of the open volumetric air receiver needs to be addressed. The presented details are both encouraging and alarming, addressing some of the gaps and outlining the need of an in-situ cleaning approach for operating such a system in the arid deserts of India and worldwide.

Keywords:open volumetric air receiver, solar convective furnace, dust deposition, heat flux distribution

1 Introduction

Rajasthan and Gujarat in India are prosperous in terms of direct normal irradiance. This can be converted to heat or power using the concentrated solar thermal technologies. As an application, the concept of solar convective furnace system is being developed at IIT Jodhpur (Patidar et al., 2015). A three-dimensional view of this furnace for heat treatment of aluminum is shown in Fig. 1a. Here, the obtained hot air from an open volumetric receiver is introduced limiting the required temperature to 750 K for annealing of aluminium. The open volumetric air receiver based central receiver systems fulfill the same and even beyond 750 K (Romero et al., 2002). The desired volumetric heating effect may be manifested by applying a uniform heat flux throughout the absorber length. In such a case, the absorber temperature at the inlet will be lower than that of the outlet. Achieving such an ideal operating condition on the field condition is not possible. This is referred to non-volumetric heating and is a manifestation of heat flux non-uniformity along the axial and radial direction. For evaluating an open volumetric air receiver, which is open to atmosphere, the solar air tower simulator facility is installed at IIT Jodhpur as depicted in Fig. 1b. The porous absorbers of this receiver are exposed to concentrated solar irradiance with simultaneous cooling basing on the forced convection of air. The installed foot-piece, anchor-plate and nozzle ensure thermal uniformity of hot air at its outlet. The designed receiver aims to provide (a) a uniform outlet air temperature, (b) a stable flow condition and (c) the long-term operation in dusty environment. An open volumetric air receiver comprising of circular straight pore based cylindrical absorber is developed to fulfill these requirements, as far as possible, and is discussed subsequently. A review and challenges in achieving the volumetric effect in such a receiver is presented in e.g. (Gomez-Garcia et al.,2016; Capuano et al., 2015).

Even with volumetric or more so with a non-volumetric heating the desired stable flow limits the targeted high air temperature in an open volumetric air receiver (Kribus et al., 1996; Pitz-paal et al., 1997). The combined effect of high temperature and its non-uniformity leads to flow instability beyond a critical heat

© 2017. The Authors. Published by International Solar Energy Society
Selection and/or peer review under responsibility of Scientific Committee
doi:10.18086/swc.2017.04.14 Available at http://proceedings.ises.org

flux level. This is associated with the thermo-physical properties of air and in particular, the offered flow resistance at a high temperature. The concentrated solar irradiance on the open volumetric air receiver aperture is known to be quasi-Gaussian and thus centrally located absorbers are more prone to such an unwanted situation (Becker et al., 2006; Roldán et al., 2014). One way of mitigating the same is the use of an absorber with high thermal conductivity to reduce thermal gradient and the resulting change in fluid properties. Another challenge pertaining to its operation in the arid desert region is the deposition of dust having a low thermal conductivity of about 1-2 W/mK in absorber pores. This is likely to limit its installation in such areas of high potential, worldwide, and in particular the Thar-desert of India and the great desert of Middle-East. The deposition mechanism and a dust removal process were analyzed by Singh et al., (2016). The possible consequences of dust deposition are (a) the flow instability even at a low heat flux concentration, (b) the local or wide-area hot spot and (c) an eventual failure of open volumetric air receiver. Considering these aspects (a) the effect of uniform and non-uniform heat flux distribution on an absorber pore and (b) the detrimental consequences of the dust deposition in an absorber pore are discussed in this paper.

(a) **(b)** **(c)**

Fig. 1: (a) Schematic of solar convective furnace,(b) Solar air tower simulator facility at IIT Jodhpur, (c) Schematic of an open volumetric air receiver

2 Modeling and simulation

In this section the derived new pressure-drop coefficient based correlation is presented. Subsequently, the validated two-dimensional computational approach is used to address the above-mentioned objectives.

2.1 Pressure-drop Correlation

The porous absorbers in an open volumetric air receiver are made of metals, alloys and ceramics that are of foam or straight pore –type (Avila-Marin, 2011). The straight two-dimensional pore based absorbers offers a lower pressure-drop in comparison to that of a three-dimensional structures, which can be easily inferred in comparison to the Ergun equation. Thus, the straight pore based receiver is attractive for pressure-drop and are also less prone to the dust accumulation. There are a number of correlations to predict the pressure-drop (Δp) across the foam-type absorbers, which may not be applicable for the straight pore based absorber (Edouard et al.,2008). Therefore, several experiments and detailed analysis are performed to deduce a realistic correlation for Δp across the designed circular straight pore based open volumetric air receiver (Sharma et al., 2015a, 2015b). The employed cylindrical absorber and the receiver assembly are shown in Fig. 2b and 2c. The schematic of experimental setup for measuring the pressure-drop across an isolated absorber is shown in Fig. 2a. This consists of a blower, two connecting pipes each of length ~0.83 m, an absorber of length (L) ~0.0254 m, pore hydraulic diameter (d_p) ~0.002 m and porosity (ε) ~52%, a differential pressure transducer (Dwyer 475 mark III with an accuracy of about ±1.5%, a rotameter and a hot-wire anemometer (Fisher scientific make with an accuracy of about ±1%). The detailed analysis is presented in Singh et al. (2018). The authors' have also reported three dimensional numerical analyses with absorbers having porosities of 42, 52 and 62%. The obtained correlation based on these investigations is as follows:

$$\left.\begin{aligned} \Delta p &= k_p \times \frac{\rho_f \mathrm{v}_p^2}{2} \\ k_p &\approx 179.25 Re_p^{-0.588} \end{aligned}\right\} \qquad \text{(eq. 1)}$$

where,k_p is the pressure drop coefficient, ρ_f is the density of air, Re_p is the Reynolds number based on the hydraulic diameter (d_p) of circular straight pore and v_p is the average speed of air inside an absorber pore. The derived correlation is expressed in terms of Re_p, which includes fluid properties. It is well known that $\left(\Delta p/\rho_f v^2\right) \propto f\left(Re_p\right)$ for an incompressible fluid flow in a smooth straight pore (Fox et al., 2011). This can be also be inferred from the fact that a blower of large capacity is required to achieve a high mass flow rate through a given porous geometry. Thus, with the increasing velocity/mass flow rate of air or the corresponding Reynolds number the pressure-drop increases. This is also evident from eq. (1) in which including the proportionality constant k_p (a function of Reynolds number) the pressure drop scale with $v^{1.412}$.

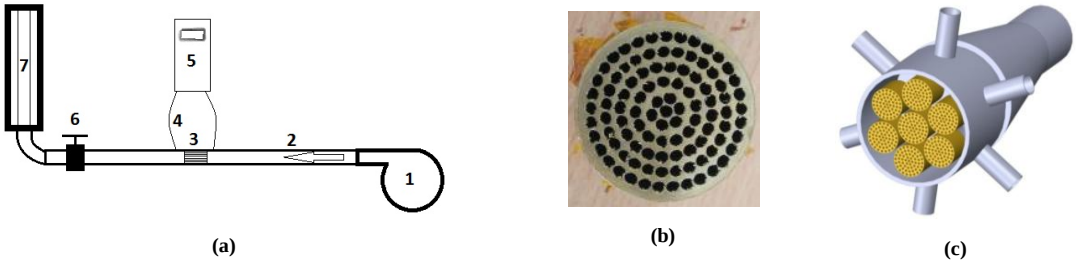

(a) (b) (c)

Fig. 2: (a) Schematic of experimental setup showing 1:blower, 2:pipe, 3:absorber, 4-5:differential pressure transducer with probes, 6:valve, 7:rotameter; (b) a circular straight pore based cylindrical absorber; (c) the receiver assembly.

2.2 Two-dimensional analysis: clean and partially blocked pore

The deposition of dust will enhance the thermal resistance in an absorber pore and as a consequence the temperature difference between solid and air will be higher than that of a clean pore. The thermal resistance between solid and air for a clean and partially blocked pore can be easily estimated as follows:

$$\left.\begin{aligned} R_{th\_cl} &= \frac{1}{h_{cl} A_{ps\_cl}} \\ R_{th\_bl} &= \frac{1}{h_{bl} A_{ps\_bl}} + \frac{\ln\left(d_{cl}/d_{bl}\right)}{2\pi k_d L} \end{aligned}\right\} \qquad \text{(eq. 2)}$$

where, R_{th} is the thermal resistance in the pore, h is the convective heat transfer coefficient in the pore, A_{ps} is the wetted surface area of the pore, d is the hydraulic diameter of the pore, subscripts *cl* and *bl* stands for clean and blocked pores, L is the length of the circular straight pore and k_d is the thermal conductivity of dust. In eq. (2) the offered conductive resistance by the absorber solid material is ignored basing on its high thermal conductivity (~ 100 W/mK) in comparison to that of dust (~ 1-2 W/mK). The porosity (ε) of absorber in terms of dust layer thickness can be obtained as

$$\varepsilon = \frac{A_c \times n_c + A_b \times n_b}{A_{cs}}, \text{where } A_c = \frac{\pi d_p^2}{4} \text{ and } A_b = \frac{\pi (d_p - 2t)^2}{4} \qquad \text{(eq. 3)}$$

where, A_c is the cross section area of a clean pore, A_b is the flow cross section area of a partially blocked pore, t is the thickness of dust layer, n_b is the number of partially blocked pores, n_c is the number of clean pores and A_{cs} is the cross section area of absorber. Therefore, if dust deposits then the porosity of absorber will be lower than that of a clean pore. This will offer higher resistance to flow and heat transfer for a given mass flow rate. For a simple analysis the uniform layer of deposited dust along the pore length is assumed. Because of the identical geometry only one pore will suffice to estimate its effect on the heat transfer. This is manifested as the rise of mean temperature difference between absorber material and air with thickness of dust layer as summarized in Table 1. The digits are rounded off to the first decimal point. In these calculations an average convective heat transfer coefficient is used, which ideally should vary along the length. Thus, the numbers are only representative in nature. The Table 1 confirms that the mean temperature difference between absorber solid and air will increase with the dust layer thickness as a result of the enhanced conductive resistance and decrease with

Re_p as a consequence heat transfer coefficient for a given thickness of dust layer. Thus the need for a more detailed analysis is realized. As the next step, a two-dimensional analysis, based on axisymmetry is performed with Ansys-Fluent.

Tab. 1: Mean temperature difference between solid and fluid in a partially blocked pore with a uniform dust layer thickness

Re_p	Dust layer thickness (Porosity in %)		
	100 µm (42%)	200 µm (33%)	300 µm (25%)
100	103.5 K	104.7 K	106.3 K
200	92.8 K	94.8 K	97.2 K
300	84.7 K	87.1 K	89.8 K

Assuming that all the pores are identical and are exposed to the same condition suffices modeling a single pore. The modeled single pore geometry comprises a fluid (air) domain with temperature dependent properties and a solid (brass) domain with constant thermo-physical properties for a clean pore. For a partially blocked pore the dust layer is introduced as a solid domain with thermo-physical properties of sand. This is sandwiched between the absorber and fluid domain (see Fig. 3a). Thus the dust-air and dust-solid interface is suitably modeled with consistent thermal boundary condition. The deposition of dust, in an ideal case, will be uniform along the length, however, in reality, a non-uniform profile is expected. To simulate these different scenarios, uniform dust layer (UDL) and non-uniform dust layer (NDL) distributions are assumed (Fig. 3a). Moreover, both the ideal volumetric and real non-uniform heating effects are modeled with uniform and non-uniform heat flux distribution on the circumference of pore. The solved continuity, momentum and energy equations are given in eq.(4) and the numerical setup is summarized in Table 2. This describes the adopted numerical scheme and the convergence criteria.

Fluid (air)

$$\nabla \cdot \vec{\mathrm{V}} = 0$$

$$(\vec{\mathrm{V}} \cdot \nabla)\,\vec{\mathrm{V}} = -\frac{\nabla p}{\rho_f} + \nu_f\ \nabla^2\,\vec{\mathrm{V}}$$

$$\left(\nabla \cdot \rho_f\ \vec{\mathrm{V}} \mathrm{H}_f\right) = \nabla \cdot \left(\frac{k_f}{c_{pf}} \nabla H_f\right)$$

Solid (absorber material/dust)

$$\nabla \cdot (k_s \nabla T) = 0$$

(eq. 4)

Tab.2: Numerical setup for two dimensional analysis

Mesh-type	**Mesh-size (in mm)**	**Numerical Scheme**	**Convergence**
Structured	0.015 mm -0.05 mm	First-order Upwind with SIMPLE algorithm	10^{-6}

The schematic in Fig. 3c and depicts (a) volumetric heating effect with a uniform heat flux and (b) non-volumetric heating effect or a field condition with a non-uniform heat flux distributions along the axial direction, ignoring the radial variation with a single pore. The latter is adopted from Roldán et al.(2014) as eq. (5) and is implemented as a user-defined function.

$$I(z) = I_0 e^{-\xi z} \text{ with } \xi_{3d} = \frac{3(1-\varepsilon)}{d_p} \qquad \text{(eq. 5)}$$

where, I(z) is the heat flux at a given axial position along the flow direction, I_0 is the irradiance at the front face, ε is the porosity of an absorber, ξ_{3d} is the extinction coefficient (Wang et al, 2013; Wu et al, 2011). Also, the

radiation based heat loss from the front surface of absorber is introduced as a boundary condition using a user defined function. Different cases are analyzed with a dust layer thickness up to 200 µm depicting one to four successive layers of deposition (see Yadav et al., 2014). Each absorber pore is subject to the same Δp inferring the applied same suction by a blower. This assumes that a common blower for suction through a receiver comprise of several porous absorbers. The same is depicted with a schematic of a clean and a partly blocked pore in Fig. 3b. In the two-dimensional simulation, a total pressure of 15.8 Pa corresponding to $\dot{q}/\dot{m}_a$~200 kJ/kg for a power ($\dot{q}$) of 1.03 W is employed as the inlet boundary condition. Zero gage pressure is applied at the outlet. Thus the flow inside a clean and a partially blocked pore is driven by the same pressure-drop as in a real absorber. The resulting Re_p is about 175, 70 and 19 for the clean and partially blocked pores with uniform dust layer thickness of 100 µm (ε ~ 42%) and 200 µm (ε ~ 33%), respectively. The lower value of Re_p is a manifestation of the offered higher resistance to the flow by the blocked pore in comparison to the considered clean pore. Thus, the flow and thermal development length (~0.05 Re_p with Pr ~ 1) will be shorter in the partially blocked pore as compared to its clean counterpart. In realistic conditions, the dust deposition is generally non-uniform. To estimate the effect of such a distribution, the simulations with non-uniform dust layers are also performed. Here, the dust layer thickness is maximum (100 µm or 200 µm) at the inlet and reduces to zero at the outlet as shown in Fig. 3a.The generated coarse and fine meshes in a dust deposited pore are shown in Fig. 3e. The finest mesh having a resolution of 0.05 mm is preferred for further analysis based on a grid independence test.

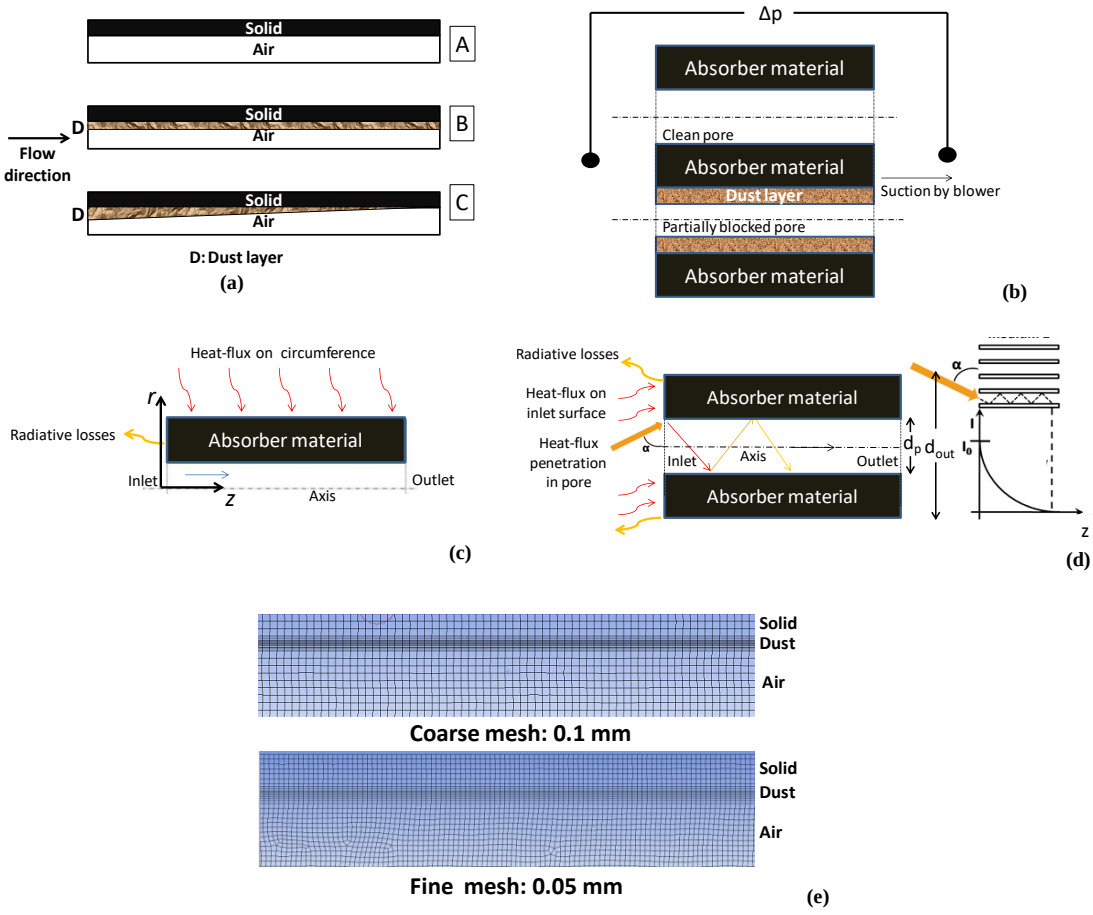

Fig. 3: (a) Geometries of A- clean pore, B.-pore with uniform dust layer (UDL), C- pore with non-uniform dust layer; (b) A schematic showing the same pressure drop across all absorber pores due to suction (c) Uniform distribution of heat flux on an absorber pore and (d) Non-uniform heat flux distribution on an absorber pore; (e) The generated meshes

3 Results and discussion

3.1. Two-dimensional analysis:validation and flow-instability with dust deposition

The employed axisymmetric numerical model is validated with the measured values of air temperature at the absorber outlet (T_{out}) with uniform or volumetric-type heating in laboratory bySharma et al., (2015a, 2015b). The comparative assessment in Fig. 4a shows a variation of less than 5% between the measured and computed values confirming the acceptability and quality of the performed analysis. The pressure-drop correlation as in eq. (1) is derived using experiments/computations under ambient condition and its applicability with heat input remains a question. To answer the same, simulations are performed using the validated numerical setup with uniform heat flux boundary conditions and Re_p < 300. A comparison between the computed and correlation based Δp is shown in Fig. 4b. This depicts that (a) the Δp increases with decreasing T_{out} that corresponds to a high mass flow rate of air or Re_p, (b) the derived correlation compares within 10-25% with the performed simulations for a T_{out} up to 900 K. One of the reasons for this error is the measurement uncertainty of about 2 Pa. This is substantial at a low mass flow rate and thus, differences are observed between experiment and computed values. Furthermore, the measured values will be affected by the curved streamlines at the inlet and outlet. Also, a comparison between the installed- rotameter and hot-wire anemometer based $\dot{m}_a$ values showed an uncertainty of about *5%*. These are some of the possible encountered errors. Also it is noted that a 5% of uncertainty in $\dot{m}_a$ corresponds to 10% uncertainty in pressure drop. Thus, the realistic pressure-drop correlation with its known limitations is used for flow stability analysis.

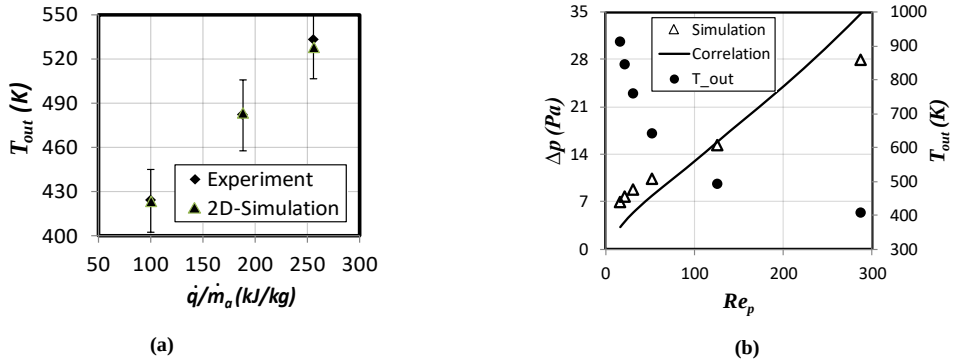

Fig 4: Comparison between (a) computed and measured air temperature at the absorber outlet and (b) computed and correlation (eq. (1)) based pressure-drop with different heat flux condition

For flow stability analysis the well-known quadratic pressure across the absorber is deduced by adopting the approach from Becker et al. (2006) and is presented in eq. (6). The detailed derivation of this expression considering a clean circular straight pore and the underlying assumption are reported in Singh and Chandra (2018). The instability is envisaged by the oscillatory nature of the difference between quadratic pressure-drop at a critical heat flux level. The investigation of the obtained expression clearly show that the non-existence of the same. The effect of dust deposition may be implicitly evaluated by updating the porosity of a partially blocked pore in eqn. (6) at the steady state.

$$\Delta p^2 = p_{inlet}^2 - p_{outlet}^2 = B'.\left(\frac{q_s''/\varepsilon\, T_{out} - \Sigma\beta\sigma T_{out}^5}{(T_{out} - T_0)}\right)^{1.412} \quad \text{where B}'=\left(\frac{179.25R\mu_0^{0.588}}{c_{pf}^{1.412}d_p^{0.588}T_0^{0.412}}\right) \qquad \text{(eq. 6)}$$

A variation of the derived expression for Δp^2 as in eq. (6) with respect to T_{out} and $\dot{m}_a$ is shown in Fig. 5. This illustrates that the pressure-drop decreases with mass flow rate of air or the corresponding Reynolds number for a circular straight pore. As a result, the outlet air temperature increases for the considered temperature dependent thermo-physical properties of air. Unfortunately, the analysis is not performed for the large scale receiver as the absorber design needs to be optimized. The work on the same is in progress. It is also inferred that for a given T_{out} the Δp^2 increases with the dust layer thickness or the decreasing effective absorber porosity

at a given mass flow rate of air. This is indicated by a dotted arrow. It must be emphasized that the estimated value of Δp^2 with eq. (6) compares well with that of the numerically analyzed values. This serves as an alternative validation of the derived expression. The difference between analytically and numerically obtained values of Δp^2 decreases with the mass flow rate of air, which is also inferred with the increasing values T_{out}. This is desirable in view of analyzing the flow instability. Higher values of Δp will lead to an elevated parasitic loss and the reduction in an overall efficiency, which is defined by Boddupalli et al. (2017). Thus, one of the consequences of dust deposition is the reduction of open volumetric air receiver performance or efficiency. Interestingly, with the uniform layer of dust deposition and the manifested volumetric heating effect no signature of flow instability is found, which is encouraging for implementing such a receiver design in desert regions and is a step towards optimization. The effect of non-uniform- dust deposition and heat flux distribution on the same will be investigated at a later date.

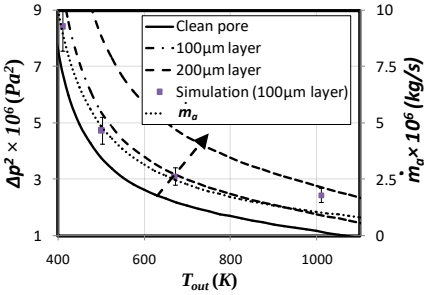

Fig. 5: Computed and eqn. (2) analyzed Δp^2 with clean and partly blocked pores.

3.2. Effect of dust deposition and heat flux distribution: air and absorber temperature

The simulations are performed with the clean and partly blocked absorberpores with an imposed fixed pressure drop across the absorber inlet and outlet (see Fig. 3b). This will allow one-to-one comparison between a clean and a partially blocked pore that are operating under an identical suction. The axial temperature variation of fluid and absorber material is shown in Fig. 6 for the cases with uniform and non-uniform heat flux distributions.

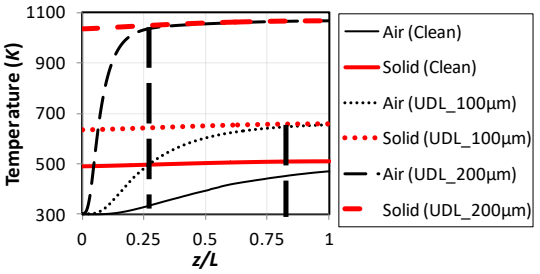

(a) Uniform heat flux(uniform dust layer, UDL)

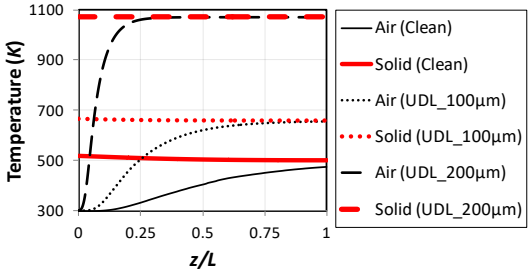

(b) Non-uniform heat flux(uniform dust layer, UDL)

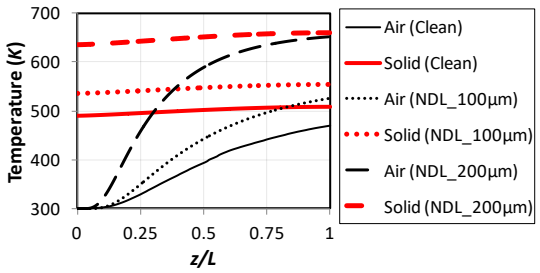

(c) Uniform heat flux (non-uniform dust layer, NDL)

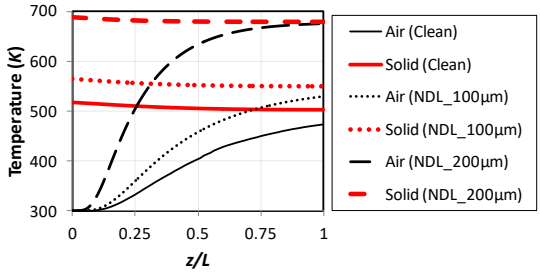

(d) Non-uniform heat flux (non-uniform dust layer, NDL)

Fig. 6: Axial temperature profile of fluid and solid with uniform and non-uniform dust layer thickness along the absorber pore

With the numerically imposed uniform heat flux along the pore length the desired volumetric heating effect is observed. This is inferred with an increasing solid temperature from the absorber inlet to outlet. Whereas with the employed non-uniform heat flux distribution along the pore length as in eq. (5) the highest absorber temperature is obtained at the inlet. This confirms the non-volumetric heating effect. The partially blocked pore shows a substantial increment in temperature with the applied pressure-drop attributed to the reduced mass flow rate. The temperatures of solid and air increase with the thickness of dust layer as expected. For the uniform dust layer a temperature rise of about 150 K and 580 K is found, which correspond to the thickness of 100 µm and 200 µm, respectively. For the non-uniform thickness of dust layer a temperature rise of about 40 K and 150 K is found, which correspond to 100 µm and 200 µm at the inlet, respectively. This is attributed to the decreasing mass flow rate of air in blocked pore for the applied pressure-drop and is substantiated by a shorter thermal development length (~ 0.05 Re_pPr) in blocked pore compare to its clean counterpart as depicted by the dotted vertical lines in Fig. 6a. Thus, it is concluded that the dust deposition is detrimental to long-term sustainable operation and also increases parasitic losses. Moreover, high surface temperature will lead to an elevated radiation based heat loss, which adds up to the losses. In essence, both the efficiency and durability of an open volumetric air receiver will be a concern in arid deserts.

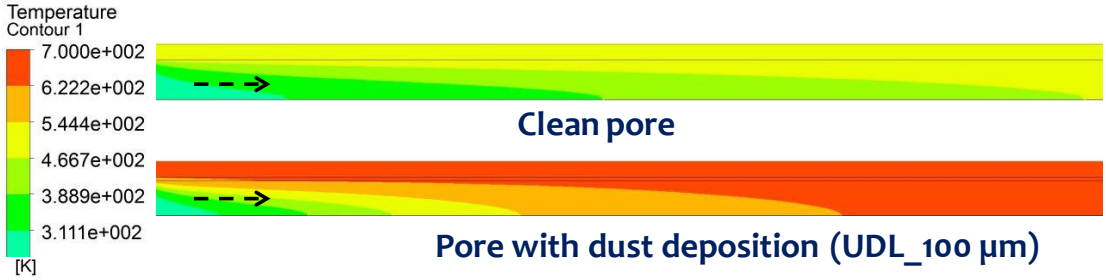

Fig. 7: Temperature contours for a clean pore and for a partially blocked with uniform dust layer (UDL) thickness of 100 µm and the applied uniform heat flux along the pore length

The numerically analyzed solid and fluid temperature contours for a clean and a partially pore is shown in Fig. 7. The scale is preserved for a better visual comparison. As observed, the contours depict parabolic distribution of fluid temperature and its value increases with the axial position. As explained in Fig. 6a, it is clear that the fluid attains the solid temperature closer to the inlet for the blocked pore case in comparison to that of the clean pore. Thus, it may be inferred that the absorber solid will be exposed to a high temperature over a wider length with the blocked pore in comparison to the clean pore under a given operating condition. Thus, the need of in-situ cleaning is a must for mitigating the failure of such a system in arid deserts.

4 Conclusions

This paper aims at demonstrating the detrimental effect of dust deposition in an absorber pore of an open volumetric air receiver. A validated two-dimensional numerical approach is adopted for this purpose. The analyses reveal the following:

a. The uniform dust deposition may not encourage flow instability in the considered absorber. This is encouraging and allows expecting a stable operation of such a receiver in desert regions.

b. The dust deposition will increase parasitic and radiation based losses that are detrimental to overall efficiency of such a receiver. These can be easily inferred from the reduced pore diameter based Reynolds number and the computed higher temperature with a partially blocked pore in comparison to a clean pore.

c. The dust deposition will lead to an elevated temperature and thus the flow resistance. This will limit the operation of such a receiver in desert regions and confirms the need of an in-situ cleaning device.

5 Acknowledgements

The authors are thankful to Ministry of New and Renewable Energy (MNRE), Ministry of Human Resource Development (MHRD) and Indian Institute of Technology, Jodhpur (IITJ) for the provided financial and infrastructural support.

6. Nomenclature

c_{pf}	Specific heat at constant pressure for air (J/kgK)	Re_p	Reynolds number in an absorber pore
d_p	Hydraulic diameter of the pore (m)	T	Temperature (K)
H_f	Total enthalpy (J)	T_0	Temperature of air at the inlet of an absorber (K)
I	Heat flux along the z-direction (W/m^2)	T_{out}	Temperature of air at the outlet of an absorber (K)
I_0	Heat flux on the inlet surface of absorber (W/m^2)	$\vec{V}$	Velocity of fluid (m/s)
k_p	Pressure-drop coefficient (-)	v_p	Average speed in an absorber pore (m/s)
k_f	Thermal conductivity of fluid (W/mK)	ε	Porosity of absorber
L	Length of absorber (m)	ξ	Extinction coefficient (m^{-1})
$\dot{m}_a$	Mass flow rate of air (kg/s)	ρ_f	Density of air (kg/m^3)
p	Static pressure (Pa)	μ_0	Dynamic viscosity of air at inlet of absorber (kg/ms)
$\dot{q}$	Power on aperture (W)	Σ	Emissivity of brass
q''_S	Concentrated solar irradiance on the receiver aperture (W/m^2)	σ	Stephan-Boltzmann constant (W/m^{2}K^4)
R	Gas constant of air (J/kgK)		

7. References

Avila-Marin, A.L., 2011. Volumetric receivers in solar thermal power plants with central receiver system technology: a review. Solar energy 85(5), 891-910.

Becker, M., Fend, T., Hoffschmidt, B., Pitz-Paal, R., Reutter, O., Stamatov, V., Steven, M., Trimis, D., 2006. Theoretical and numerical investigation of flow stability in porous materials applied as volumetric solar receivers. Solar energy 80(10), 1241-1248.

Boddupalli, N., Singh, G., Chandra, L., Bandyopadhyay, B., 2017. Dealing with dust-Some challenges and solutions for enabling solar energy in desert regions, Solar Energy 150, 166-176.

Capuano, R., Fend, T., Hoffschmidt, B., Pitz-Paal, R., 2015. Innovative volumetric solar receiver micro-design based on numerical predictions. In ASME 2015 International Mechanical Engineering Congress and Exposition (Vol. 8, pp. 13-19).American Society of Mechanical Engineers.

Edouard, D., Lacroix, M., Huu, C.P., Luck, F., 2008. Pressure drop modeling on solid foam: State-of-the art correlation. Chemical Engineering Journal 144(2), 299-311.

Fox, R., McDonald, A., Pritchard, P., 2011. Fluid Mechanics. 8thed. New York: Wiley.

Gomez-Garcia, F., González-Aguilar, J., Olalde, G., Romero, M., 2016. Thermal and hydrodynamic behavior of ceramic volumetric absorbers for central receiver solar power plants: A review. Renewable and Sustainable Energy Reviews 57, 648-658.

Kribus, A., Ries, H., Spirkl, W., 1996. Inherent limitations of volumetric solar receivers.Journal of solar energy engineering 118(3), 151-155.

Patidar, D., Tiwari, S., Sharma, P., Pardeshi, R., Chandra, L., Shekhar, R., 2015.Solar Convective Furnace for Metals Processing. JOM 67(11), 2696-2704.

Pitz-Paal, R., Hoffschmidt, B., Böhmer, M., Becker, M., 1997.Experimental and numerical evaluation of the performance and flow stability of different types of open volumetric absorbers under non-homogeneous irradiation. Solar Energy 60(3), 135-150.

Roldán, M.I., Smirnova, O., Fend, T., Casas, J.L. Zarza, E., 2014. Thermal analysis and design of a volumetric solar absorber depending on the porosity. Renewable Energy 62, 116-128.

Romero, M., Buck, R., Pacheco, J.E., 2002.An update on solar central receiver systems, projects, and technologies.Journal of solar energy engineering 124(2), 98-108.

Sharma, P., Sarma, R., Chandra, L., Shekhar, R., Ghoshdastidar, P.S., 2015a. Solar tower based aluminum heat treatment system: Part I. Design and evaluation of an open volumetric air receiver. Solar Energy 111, 135-150.

Sharma, P., Sarma, R., Chandra, L., Shekhar, R., Ghoshdastidar, P.S., 2015b. On the design and evaluation of open volumetric air receiver for process heat applications. Solar Energy 121, 41-55.

Singh, G., Dhurwe, P., Kumar, R., Kumar L., Vaghela, N., Chandra, L., 2018. A step towards realizing open volumetric air receiver based systems in desert regions, Springer Proceedings in Energy, ICAER 2017 (to appear).

Singh, G., Chandra, L., 2018. On the flow stability in a circular cylinder based open volumetric air receiver for solar convective furnace. Energy Procedia, In: HEREM 2018 (To appear)

Singh, G., Saini, D., Chandra, L., 2016. On the evaluation of a cyclone separator for cleaning of open volumetric air receiver, Applied Thermal Engineering 97, 48-58.

Wang, F., Shuai, Y., Tan, H., Yu, C., 2013. Thermal performance analysis of porous media receiver with concentrated solar irradiation, Int. J. Heat and Mass Transfer 62, 247-254.

Wu, Z., Caliot, C., Flamant, G., Wang, Z., 2011.Coupled radiation and flow modeling in ceramic foam volumetric solar air receivers, Solar Energy 85(9), 2374-2385.

Yadav, N.K., Pala, D., Chandra, L., 2014. On the understanding and analyses of dust deposition on heliostat, Energy Procedia 57, 3004-3013.